Potential of Weathered Blast Furnace Slag for use as an Addition in Concrete

Dyer, Thomas D.; McCarthy, Michael J.; Csetenyi, Laszlo J.

Published in:
Magazine of Concrete Research

DOI:
10.1680/jmacr.19.00142

Publication date:
2021

Document Version
Peer reviewed version

POTENTIAL OF WEATHERED BLAST FURNACE SLAG FOR USE AS AN ADDITION IN CONCRETE

T D Dyer[1], M J McCarthy[1] and L J Csetenyi[1]

Keywords: **Cement/cementitious materials, Chemical properties, Sustainability**

Word: 5123 (Excluding Abstract and References)
Tables: 5
Figures: 11

[1]Concrete Technology Unit
Civil Engineering
School of Science and Engineering
University of Dundee
DD1 4HN
Scotland, UK

Contact: m.j.mccarthy@dundee.ac.uk
Tel: +44 1382 384924
Fax: +44 1382 384389

Potential of Weathered Blast Furnace Slag for Use as an Addition in Concrete

T D Dyer, M J McCarthy and L J Csetenyi

Abstract
The paper investigates the potential for recovering granulated blast furnace slag after four years storage in a stockpile (weathered) for use as an addition in concrete. The initial research physically and chemically characterized fresh and weathered granulated slag. Thereafter, studies on ground materials, including their use in paste and mortar were carried out. The weathered granulated slag was similar to fresh slag in terms of particle size, shape and elemental composition. However, there was greater roughening of particle surfaces, with various weathering products forming. Following grinding, fresh slag comprised angular particles covering a range of sizes, while finer particles in weathered slag included fragmented reaction products. In cement paste, weathered slag gave reductions in chemically bound water. In mortar, this showed little difference in flow properties compared to fresh slag, with reductions in compressive strength and increases in porosity also noted. Further analyses suggest that, at equal Blaine fineness, weathered slag (i) is actually coarser than fresh material, affecting particle packing and giving larger capillary pores, and (ii) has lower reactivity due to reduced surface area. The practical implications are examined and approaches to using weathered slag in concrete suggested.

1. INTRODUCTION

The use of additions (cement components) in concrete, particularly ground granulated blast furnace slag (GGBS), from iron production, and fly ash, from coal-fired power generation, with Portland cement (PC), mainly developed during the latter part of the 20th Century. These materials can offer several benefits to concrete, including reduced heat evolution, and enhanced long-term strength and durability properties (Paine *et al*, 2006; Thomas, 2013; Dyer, 2014). More recently, their role in reducing embodied CO_2 in the material (Mineral Products Association, 2015) and conserving mineral resources has been noted (Concrete Society, 2011). The above effects and expected growth in cement requirements worldwide (Favier *et al*, 2018) mean their demand is expected to increase.

At the same time, however, with re-organisation in the iron and steel industry (Rhodes, 2018) and planned coal-fired power station closures (McCarthy *et al*, 2017) in the UK, the availability of GGBS and fly ash are likely to be affected. One of the options that has been identified for sourcing these in future is material from stockpiles (BEIS, 2017). While the use of fly ash from these storage areas has received increasing attention (Robl *et al*, 2006; McCarthy *et al*, 2018) with greater quantities available for recovery (BEIS, 2017), less is known about GGBS held in this way.

Granulated slag is produced by tapping off liquid slag from the blast furnace with rapid cooling in a water stream, giving mainly amorphous granules. These are typically stockpiled before grinding to a fine powder for use as an addition (CCA Australia, 2018). This period depends on market conditions, but with time wet-storage can lead to weathering – sometimes referred to as 'pre-hydration' – a process influenced by factors including temperature/moisture conditions and material properties (Matthes *et al*, 2017). This may affect the slag properties and its use in concrete (Battagin and Peccio, 2003; CCA Australia, 2018). While weathering of blast furnace slag has received little attention, more information is available for steel slags (e.g. Yildirim and Prezzi, 2015; Jianga *et al*, 2018). Although these differ compositionally (e.g. iron, glassy and crystalline contents) (Scott *et al*, 1986; Yildirim and Prezzi, 2011), a comparison of weathering for both slags can enable certain effects to be identified or inferred.

In steel slag, larnite (also found in PC and hydraulic limes) reacts with water, forming calcium silicate hydrate (CSH) phases and portlandite ($Ca(OH)_2$; lime will also hydrate, giving portlandite). These may react with atmospheric carbon dioxide in the presence of water giving calcium carbonate (and silica gel, for calcium silicate hydrates) (Mayes *et al*, 2018). The glassy components of blast furnace slag can also form calcium silicate – or calcium aluminosilicate – hydrates (CASH) in contact with water, albeit at a much slower rate, and again, are likely to carbonate in contact with air. Given the potential of weathered stockpiled blast furnace slag as an addition in concrete, a study was devised to examine this. The research compared the characteristics of weathered blast furnace slag with fresh (unweathered) material, before investigating reactivity and fresh/hardened properties in paste and mortar, once finely ground.

2. MATERIALS

2.1 Granulated Blast Furnace Slag

The granulated blast furnace slag used during the study was obtained from a source in mainland Europe. The weathered slag had been exposed at the site to external conditions in a stockpile for 4 to 5 years, before drying in laboratory air, thereby preventing further weathering. The unweathered slag was similarly dried, shortly after granulation. This material is referred to as 'fresh slag' in the subsequent text.

After examination of the intact granules using scanning electron microscopy (SEM), sub-samples were prepared as follows:

(i) Fresh slag was ground to a Blaine fineness of 3800 cm^2/g;

(ii) Weathered slag was ground to the same Blaine fineness – 'Weathered Slag 1 (WS1)';

(iii) Weathered slag was ground for 2 minutes longer than WS1 – 'Weathered Slag 2 (WS2)'.

Blaine air permeability measurements (BS EN 196-6, 2018) were used to determine fineness, given its wide use in the cement industry and practical relevance. Grinding was carried out in a planetary ball mill in 300 g batches, with 10 mm and 5 mm diameter steel balls. The slags were initially ground for 30 minutes with the 10 mm balls and then with the smaller balls until achieving the required Blaine fineness. The fresh slag required 40 minutes in total, whilst for WS1 and WS2 grinding times of 42 and 44 minutes, respectively, were used.

2.2 Other Materials

The PC was a CEM I of Strength Class 52.5 N to BS EN 197-1 (BSI, 2011). Its physical and chemical properties (from the supplier) are shown in Table 1. Standard (CEN) sand to BS EN 196-1 (BSI, 2016) was used in the test mortars for measuring flow characteristics and compressive strength.

3. PREPARATION OF PASTE AND MORTAR

Paste samples of 0.5 w/c ratio comprising 50% PC and 50% slag by mass were prepared by hand mixing to investigate hydration product formation and chemically-combined water for the various slags. At an age of 28 days, these specimens were broken up using a percussion mill and subsequently ground to a powder with a mortar and pestle. Hydration was arrested by dispersing this in acetone for 60 minutes before filtering and drying the residue in a vacuum oven at 45°C for 5 hours.

Mortar was prepared following BS EN 196-1 (BSI, 2016) with 50% PC/50% slag by mass. The mortar mixes comprised 225 g PC, 225 g slag, 1350 g sand and 225 g water. In addition, a PC control mortar was prepared using 450 g PC. These were used for fresh and hardened property tests.

Following the initial 24 hours under damp hessian and polythene sheets, curing of the hardened pastes and mortars was carried out in water at 20°C until testing.

4. EXPERIMENTAL PROCEDURES

4.1 Physical and Chemical Characteristics and Weathering Products

SEM was used to examine the morphology of the slag materials (Hitachi S-4700 instrument, operating at an accelerating voltage of 5–15 kV). Samples were prepared by depositing material on a 10 mm diameter adhesive tape/aluminium stub, coated with a 25 nm layer of palladium–gold alloy.

The chemical composition of the powdered slags was determined by X-ray fluorescence (XRF) spectrometry. The pressed pellet samples were analysed using a Panalytical Zetium 2.4 kW X-ray fluorescence spectrometer.

Blaine fineness was determined following BS EN 196-6 (BSI, 2018), using a ToniPERM 6565 automatic air permeability instrument. The results presented are averages of three measurements. BET (Brunauer – Emmett – Teller) specific surface area (SSA) was measured using a Quantachrome Nova 3000e analyser. The 4 to 5 g sample was vacuum dried before testing, by maintaining a 77 Pa vacuum and temperature of 105°C overnight. The quantity of nitrogen taken up in an adsorption and desorption cycle was then automatically determined. The particle size distribution (PSD) was measured by laser diffraction using a particle size analyser (Malvern Mastersizer 2000). Determinations of PSD were carried out on approximately 0.5 g of material added to 800 ml of water, dispersed ultrasonically prior to testing.

The fresh and weathered slags, and the hardened pastes, were analysed using powder X-ray diffraction (XRD). This used a Siemens D5000 powder X-ray diffractometer with a Cu-Kα source operating at 40 mA and 40 kV. Scans were obtained using angular increments of 0.1° 2θ at a rate of 0.33° 2θ/minute. Thermogravimetry (TG) was carried out on both ground slag and paste samples with a Netzsch STA 409 PC instrument. A heating rate of 10°C/minute was used from ambient temperature to 1000°C, whilst nitrogen was passed through the furnace at a rate of 125 ml/minute.

4.2 Properties of Mortar

Mortar spread tests were carried out using a flow table to BS EN 1015-3 (BSI, 1999). The fresh mortar was added to a brass truncated conical mould, positioned on the flow table, with compaction carried out by hand. The mould was removed and 15 jolts in 15 seconds applied. The resulting spread of mortar was measured across 4 diameters and the mean taken as the mortar flow.

The strength of the various slag materials (and PC) were measured, as described in BS EN 196-1 (BSI, 2016) and BS EN 15167-1 (BSI, 2006) on mortar prisms (40 mm × 40 mm × 160 mm). Tests were made in compression at 7 and 28 days, with three specimens at each test age giving six results (3 × 2). Longer-term tests at 90 days were also carried out, with two specimens, giving four results (2 × 2) in this case.

Porosity of the mortars was assessed by mercury intrusion porosimetry (MIP), using fragments taken from the 28-day mortar prisms, with a hammer and chisel, and dried in air to constant mass. MIP of the samples at variable pressure rates up to 230 MPa was then carried out, with pores above 6.5 nm being measured.

5. RESULTS AND DISCUSSION

5.1 Slag Granules

Figure 1 shows SEM images of fresh and weathered slag granules respectively. The granules have dimensions of several hundred microns, and are angular in nature. Bubbles are present at the fracture surfaces of the fresh slag granules. It is evident that both materials are covered in a layer of deposits of uneven texture, which appears to be thicker for the weathered material.

Figure 2 shows higher magnification images of the granule surfaces. In the case of fresh slag, the layer comprises mainly smooth, cracked material, which occasionally becomes rougher in places, with some thin, needle-shaped crystals. Similar features are seen on the weathered slag granule, although the surface is much rougher, with larger, faceted crystals present. The most likely explanation for these differences is that weathered slag has reacted to a greater extent, during its longer period of stockpile exposure. The

needle-shaped crystals are typical of those found in ettringite ($[Ca_3Al(OH)_6 \cdot 12H_2O]_2 \cdot (SO_4)_3 \cdot 2H_2O$), which may be related to the chemical composition of blast furnace slag.

Table 2 shows the chemical compositions of the fresh and weathered slags. This indicates that there is little difference in elemental composition between the materials. However, increases in loss on ignition (LOI) were noted with weathered slag, which appear to reflect hydration reactions occurring in the material (Battagin and Pecchio, 2003).

5.2 Ground Slag

The fineness of the ground slag samples using the Blaine technique and BET SSA measurements are shown in Table 3. The fresh slag and WS1 samples have similar Blaine fineness results, as expected, given the grinding procedure employed. WS2 has a Blaine fineness less than the other ground materials, albeit only slightly. This appears to reflect variability of the Blaine method, given the extended grinding time used for the latter material. The results suggest that weathering may slightly extend grinding requirements for the same fineness. In the case of the BET nitrogen adsorption tests, fresh slag had the highest SSA, followed by WS2 and WS1, albeit the differences were minor.

Figure 3 gives the cumulative PSDs of the ground slag samples, by laser diffraction. This indicates that the weathered materials are noticeably coarser than fresh slag, with WS2 slightly finer than WS1. The theoretical SSA of the ground materials, calculated from the distributions, assuming spherical particles, are given in Table 3. In terms of the ranking observed, the values are approximately in agreement with the BET SSA results. It should be recognised that the BET results can be considered the most accurate of these measurements (TRB, 2013): BET nitrogen absorption measures the mass of a monolayer of nitrogen molecules on the specimen surface, thereby reflecting particle texture, whilst Blaine fineness infers SSA from air permeability measurements.

Interpretation of the results from the three test methods is assisted by examining SEM images of the ground materials, shown in Figure 4 for the fresh and weathered slags. For fresh slag, the morphology is

predominantly angular shaped particles. More specifically, the image shows larger particles covered with smaller ones, which in turn are covered with still smaller particles, which all appear to have similar angular morphology. This contrasts with the weathered materials, where larger particles remain angular in nature, but smaller ones appear to have a more complex, rough surface texture. These are presumably due to a proportion of the particles comprising reaction products from weathered granule surfaces.

The rougher surfaces of the smaller particles are likely to reduce air permeability of a compacted mass of powder, measured by the Blaine method. This is because the principle behind the technique assumes smooth, angular particles, typical of PC and fresh ground slag. The presence of irregular particle surfaces is likely to increase air flow resistance. This can be understood more clearly by considering Meng's deconvolution of permeability (k), taking the form:

$$k = \frac{r_e P_e^2}{S_e} \quad (1)$$

where k = permeability (m^2)

r_e = effective pore radius of the material (m);

P_e = effective porosity; and

S_e = effective internal surface area of a porous solid (m^{-1}) (Meng, 1994).

In a compacted powder, as particle size decreases, r_e will decrease, P_e will either decrease or remain unchanged, whilst S_e increases. However, the reaction products on weathered granules will add surface area, even before grinding, which may be retained following this. Thus, the weathered slag will need a smaller reduction in r_e and P_e – and, thus, a smaller decrease in particle size to achieve a comparable Blaine fineness to fresh slag. In other words, grinding fresh and weathered slags to the same Blaine fineness (i.e. as for fresh slag and WS1) is likely to give a weathered slag which is, in reality, coarser. It has also been suggested (Matthes *et al*, 2017) that as weathering products may be more readily broken down during grinding, the reactive component, after carrying this out to equal fineness, will be coarser in weathered material. Thus, in terms of the SSA results in Table 3, the BET specific surface is the more accurate of the results, but those from laser diffraction are likely to most closely represent the available surface area of unreacted (and, therefore, *reactive*) slag.

Figure 5 shows the powder XRD traces for the two slags. The main feature of both is a broad peak at an angle of around 30° 2θ, and a second, broader peak between around 45 and 50° 2θ. These are due to the glassy phases, which make up the vast majority of blast furnace slag.

There are, however, additional features on the weathered slag traces. Firstly, there are two clear peaks at 27.1 and 29.3° 2θ. Whilst the quantities are small, and the lack of a clear pattern makes unambiguous identification difficult, it is likely that these correspond to vaterite ($CaCO_3$) and calcite ($CaCO_3$) respectively. Another feature of the XRD trace for weathered slag is a broader peak between around 4.5 and 7.5° 2θ, which may indicate the presence of calcium silicate hydrates or calcium aluminosilicate hydrates. These normally display a broad peak in this region, with one at around 30° 2θ (Chang and Fang, 2015). If the latter is present, it is obscured by the broad peak from the glassy material. It should be noted that the peak between 4.5 and 7.5° 2θ is also present in the fresh material, but less pronounced.

The phases identified from the XRD trace are compatible with the features seen on slag grain surfaces. Ettringite may also be present in weathered material – a faint characteristic peak at around 9° 2θ is possibly visible – however, if this is the case, it is in very small quantities. These give general agreement with effects noted previously for wet stored material (Battagin and Pecchio. 2003).

Figure 6 shows TG and differential TG (DTG) plots from fresh and weathered slags. Whilst mass loss over the temperature range is small in both cases, this is clearly greater for weathered slag. The mass losses observed between ambient temperature and 100°C are most probably due to evaporation of free moisture. Above this temperature, mass loss observed occurs at approximately the same temperatures (170°C, 630°C and 870°C) for fresh and weathered materials and matches those noted for carbonated calcium silicate hydrate phases (Chang and Fang, 2015), corresponding to dehydration of CSH (170°C) and decomposition of calcium carbonate (630 and 870°C) as a loss of CO_2. The two temperatures for calcium carbonate decomposition reflect differences in particle sizes, with finer crystallites breaking down at a lower temperature (Webb and Heystek, 1957). Thus, the mass loss characteristics suggest a greater proportion of large calcium carbonate crystals in weathered slag, compatible with a prolonged period of

wet storage. The slags, once ground into powder, were kept in air-tight containers, but no special measures were taken to prevent weathering products from carbonating. Thus, whilst it is likely that most carbonation occurred during the weathering process itself, continuation of the process after grinding cannot be ruled-out.

In quantitative terms, the mass loss from dehydration of CSH was 0.30% and 0.45% by mass for fresh and weathered slags. This cannot be easily translated into a mass of CSH phases, since the quantity of chemically-combined water in these materials varies. However, the mass loss from calcium carbonate equates to 1.52 and 2.05% for fresh and weathered slags, respectively. The weathered sample also gives a small mass loss at around 112°C, which is probably due to dehydration of ettringite.

5.3 Ground slag in paste

XRD traces for pastes at an age of 28 days are given in Figure 7. These show the main crystalline hydration products in all pastes to be portlandite and calcium aluminate monocarbonate hydrate ($3CaO{\cdot}AlO_3{\cdot}CaCO_3{\cdot}11H_2O$), with ettringite present in the PC control paste in smaller quantities, and to a lesser extent in the slag blends.

The TG traces of PC control and PC/slag pastes are shown in Figure 8. Up to around 600°C, these give a measure of total bound water, with a greater mass loss denoting a higher quantity. A prominent feature of these is the mass loss associated with portlandite at around 450°C. The results of differentiation of the traces (DTG) are also shown. Differentiation resolves two distinct mass-loss events at around 120 and 170°C – but continuing to higher temperatures – which correspond to calcium silicate hydrate phases and calcium aluminate monocarbonate hydrate, respectively, given the latter tends to decompose at temperatures close to 200°C (Carlson and Berman, 1960). As small quantities of ettringite were seen in all of the XRD traces (with the possible exception of the PC / fresh slag blend) it is likely that the mass loss at 120°C also includes the dehydration of this phase.

The quantity of bound water increases in the sequence PC/WS1 < PC/WS2 < PC/Fresh slag < PC control.

5.4 Ground slag in mortar

Table 4 shows the flow measurements of the fresh mortar mixes for the PC control and slag materials. The mortar spread diameters of the slags were very similar, and comparable to that of the PC control. Generally, finer slag will reduce flow diameter (Page and Fanourakis, 2008). However, it is unlikely that the small differences in particle size distributions between fresh and weathered slags would give noticeable effects on flow characteristics.

Figure 9 gives the compressive strengths of the PC control and PC/slag mortars at 7, 28 and 90 days. One of the strength test results (WS1, 28 days) was discarded since it deviated by more than 10% from the mean, as required by BS EN 196-1 (BSI, 2016). The rate of strength development in the mortar containing fresh slag was consistently higher than those with weathered slag, particularly after 28 days. The strength development curves of the two weathered slag mortars were almost indistinguishable.

Figure 10 shows pore size distributions in mortar using MIP. The PC control mortar had very little porosity with a diameter > 0.2 μm, with a modal pore diameter of around 0.09 μm. The same is also true of mortar with fresh slag, although the total porosity was lower (see Table 5). The pore size distributions of the weathered slag mortars were coarser, with a modal diameter of around 0.15 μm. Both of the mortars have higher total porosities compared to those with PC and fresh slag.

6. WEATHERED SLAG BEHAVIOUR WITH PORTLAND CEMENT

SEM images, and mineralogical analysis of the slag materials investigated in this study, show that the exposure of granulated blast furnace slag to the external environment leads to chemical reactions at the surface and product formation, including amorphous material (probably calcium silicate hydrates or calcium aluminosilicate hydrates), as well as calcium carbonate phases and ettringite. These increase surface area, giving a coarser PSD when weathered slag granules are ground to a required Blaine fineness. The implications of this on subsequent performance with PC requires further elaboration.

The principal effect of differences in PSD for fresh and weathered slags ground to the same Blaine fineness is a reduced rate of strength development when combined with PC in mortar, particularly at later ages. This may reflect the higher porosity of weathered slag mortars. Moreover, the modal pore diameters of these are higher than the PC control and fresh slag mortars, which will also contribute to lower strengths (Kondraivendhan and Bhattacharjee, 2010).

It is likely that weathering and the coarsened particle size distribution from grinding weathered slag to a required Blaine fineness, has the potential to affect performance via three mechanisms:

(i) The weathering products may be less available for reaction compared to the glassy phases of the original slag, leading to weathered slag forming fewer cementitious reaction products in the presence of hydrating PC;

(ii) Coarser particles will tend to pack together with larger voids, leading to coarser porosity;

(iii) The coarser particles will have a smaller SSA of glassy material, meaning the rate of reaction of this material in the presence of hydrating PC will be lower.

It is difficult to confirm whether mechanism (i) applies from the results presented. However, given the total quantity of reaction products on weathered slag was small, this effect is likely to be minor. The influence of coarsened particle size, however, may be more pronounced.

Mechanisms (ii) and (iii) will have similar influences on total porosity and pore size distributions. In general, the pore size distribution of a granular solid will resemble the PSD, albeit pore diameters are orders of magnitude smaller than corresponding particles (Gupta and Larson, 1979). Figure 11 shows the pore size distributions of the mortars normalised with respect to the cumulative pore volume below 10 μm diameter, and calculated PSDs of PC and slag combinations in the volume ratio 48:52 (i.e. for a 50% PC/50% slag combination, assuming densities for PC of 3.15 g/cm^3 and slag of 2.90 g/cm^3). The similarity between the data sets is evident, particularly in terms of the differences between weathered and fresh slag combinations. This provides evidence for coarse pores in the original particle assemblage persisting in hardened mortar.

Determining the effect of coarser weathered slag on *total* porosity is more complex. However, it is possible to estimate the porosity of a random close packed collection of particles of continuous size distribution (which applies here) using the method of Dinger *et al* (1982). This requires the diameter ratio of finest and coarsest particles (d_0/D) and a distribution coefficient (q) using a modified Andreasen (or Albert) model (Funk and Dinger, 1994) of the form:

$$CPFT\% = 100\left(\frac{d^q - d_0^q}{D^q - d_0^q}\right) \quad (2)$$

where *CPFT%* is the percentage of cumulative particles finer than particle diameter d.

This distribution function was fitted to the calculated PSDs for the PC/slag combinations discussed above. During fitting d_0, D and q were refined giving q values of 0.377, 0.210, 0.194 for the fresh, WS1 and WS2 combinations, respectively, and d_0/D values of 0.017, 0.014 and 0.014.

Using the 'modified Westman and Hugill algorithm' proposed by Funk and Dinger (1994), a higher d_0/D value gives an increased porosity, whilst for a given d_0/D ratio, a q value of 0.37 should yield optimum packing. The theoretical porosities of the PC/slag combinations were calculated using the algorithm (except a factor of 0.4% was not applied to the result, as proposed by Funk and Dinger, since this value is somewhat arbitrary). The results obtained were 26.9, 25.7 and 25.9% for the fresh, WS1 and WS2 combinations, respectively. Thus, the theoretical initial total porosities of the combinations are very similar.

Some caution is required in drawing conclusions from this analysis. Firstly, water is present in fresh cement paste, introducing additional particle space, although the original volume of water is the same in all cases in the mortar mixes (approximately 25%) meaning this effect should be minimal. Secondly, Funk and Dinger's calculations assume no interactions between particles, which in reality is not the case. However, it is reasonable that the predicted effects on porosity broadly reflect conditions in the material. Thus, it can be deduced that the high total porosity in the weathered slag mortars is unlikely to be due to the coarser particles, but the coarser porosity *is*.

On this basis, the higher total porosities in hardened mortars containing weathered slag must be the result of mechanism (iii), since a slower slag reaction rate will reduce that at which both pore diameters and total porosity decrease due to hydration product deposition. It should be noted that calcium silicate hydrate phase formation during PC and slag reactions will reduce coarse capillary porosity between cement and slag grains, but introduce 'gel pores' in the calcium silicate hydrate phases (i.e. having a diameter of <10 nm in Table 5). However, the net effect is a decrease in total porosity. Thus, for mechanism (iii), fresh slag paste should undergo these changes more rapidly than those with weathered slag because of the higher surface area available for reaction, meaning the latter will display greater porosities and larger pore diameters.

TG analyses of the pastes provide an indication of the degree to which mechanism (iii) contributes. It may be expected that slag pastes would have less bound water than PC paste, given the reactions occurring with each. Figure 8 also shows the TG trace for PC paste scaled to represent a 50% by mass PC/50% chemically-inert material. The PC/slag pastes all contain higher quantities of bound water compared to the scaled trace, indicating the slag has reacted in all cases giving additional hydration products to those of PC. Since bound water contents of the slag pastes correlate to the slag fineness, it appears that mechanism (iii) also contributes to the higher porosities of both weathered slag mortars, and hence to the effects noted for strength development.

7. PRACTICAL IMPLICATIONS

There is likely to be growing demand for additions such as GGBS, which can give a number of benefits to concrete, not least environmental. However, the material is produced as part of another process and changes in this industry may lead to issues with supply. The future for sourcing material may see increases in international trade, with slag in long-term storage in stockpiles also providing another option. The work of the study indicates that this type of storage may give changes to the material properties, which may have implications for use in combination with PC in concrete.

The European standard for GGBS in concrete (BS EN 15167-1, BSI, 2006) uses an activity index to determine reactivity. This requires standard GGBS mortars, as used in the study, to have strengths of at least 45 and 70% that of the PC control at 7 and 28 days. All three slag types satisfied the first of these: 59, 52 and 54% for fresh slag, WS1 and WS2, respectively. However, only fresh slag satisfied the latter: 72% compared to 67 and 64% for WS1 and WS2, respectively.

As noted in the study, at an equivalent (Blaine) fineness, between fresh and weathered slag, the latter is effectively coarser and of reduced reactivity. Options for using the material as an addition in concrete could then be (i) extending the grinding period to produce suitable fineness weathered slag, or (ii) adjusting mixes, e.g. by combining fresh and weathered slag, or modifying w/c ratio, to achieve equivalent properties. It should be recognised that effects occurring with slag in stockpiles are likely to depend on the material properties and storage conditions. Hence further work is necessary to determine the influence of these factors on behaviour, as well as the requirements for (i) and (ii) above.

8. CONCLUSIONS

A comparison of freshly produced slag granules, with those undergoing weathering in a stockpile for 4 years indicate similarities between materials in terms of their shape, size and elemental composition, but differences in the surface texture deriving from the presence of a noticeably thicker layer of reaction products at the surfaces of weathered granules.

Examination of the ground materials indicates that while fresh slag comprises similar angular particles covering a range of sizes, the weathered slag also contained smaller particles of a more irregular shape, which appeared to derive from weathering products.

Some differences in ranking were noted between fineness measurements for the slag materials. For example, while the various materials had similar Blaine fineness, the BET SSAs and the laser particle size analysis indicated that the weathered slags were coarser. These effects seemed to correspond to the presence of weathering products and the bases used for the various measures of fineness.

While the bulk oxide compositions were very similar between fresh and weathered slags, an increase in LOI was noted. Mineralogical analyses indicate the presence of calcium silicate hydrate or calcium aluminosilicate hydrate, calcium carbonate phases, with traces of ettringite in weathered slag. These were either absent, or much less pronounced in the case of fresh slag samples.

Analysis of cement pastes show that the main crystalline hydration products in all pastes were portlandite and calcium aluminate monocarbonate hydrate, with ettringite present in the PC control paste in smaller quantities, and to a lesser extent in the slag blends. TG tests indicate that bound water levels at 28 days increased in the following order, PC/WS1 < PC/WS2 < PC/Fresh slag < PC control.

Mortar flow tests show little difference in this property between the various PC/slag mortars and that of the PC control. Compressive strength tests gave reductions in weathered slag mortars compared to those containing fresh slag, with differences tending to increase with time to 90 days. There was also general agreement between compressive strength and porosity for the various slag mortars. It is suggested that extended grinding or mix adjustments could be options for using weathered slag in concrete.

It should be noted that this paper reports on a study intended to obtain an initial understanding of the nature of weathering on granular blastfurnace slag and its influence on performance. Whilst blast furnace slag composition may not vary widely from source to source, further investigation of this and the effects of environmental conditions, as well as storage time, require further study.

ACKNOWLEDGEMENTS

The Authors would like to acknowledge Dr Nigel Cooke (UK Quality Ash Association) and Francis Flower for assisting in sourcing and processing the slag samples. Thanks are also given to Hanson Cement for supplying the Portland cement used and to Ms Xiaoyu Zhang for her help during the experimental work.

Notation

BET:	Brunauer-Emmett-Teller
CASH:	calcium aluminosilicate hydrate
CPFT%	percentage of cumulative particles finer than diameter d
CSH:	calcium silicate hydrate
d	particle diameter, m
D	largest particle diameter in a particle size distribution, m
d_0	smallest particle diameter in a particle size distribution, m
DTG:	differential thermogravimetry
GGBS:	ground granulated blastfurnace slag.
MIP:	mercury intrusion porosimetry
k:	permeability, m^2
PC:	Portland cement
P_e	effective porosity
PSD:	particle size distribution
q	distribution coefficient
r_e	effective pore radius, m
S_e	effective internal surface area, m^{-1}
SEM:	scanning electron microscope
SSA:	specific surface area
TG:	thermogravimetry
WS:	weathered slag
XRD:	X-ray diffraction
XRF:	X-ray fluorescence spectrometry

REFERENCES

Battagin AF and Pecchio M. (2003). Blast furnace slag weathering study. Proceedings of the 11th International Congress on the Chemistry of Cement, Durban, South Africa, 8 p.

BEIS (Department for Business, Energy and Industrial Strategy). (2017). Fly ash and blast furnace slag for cement manufacturing. BEIS research paper No. 19, Crown copyright, 33 p.

British Standards Institution. BS EN 1015-3. (1999). Methods of test for mortar for masonry. Determination of consistence of fresh mortar (by flow table). BSI, London, UK.

British Standards Institution. BS EN 15167-1. (2006). Ground granulated blast furnace slag for use in concrete, mortar and grout. Definitions, specifications and conformity criteria. BSI, London, UK.

British Standards Institution. BS EN 197-1. (2011). Cement, Part 1: Composition, specifications and conformity criteria for common cements. BSI, London, UK.

British Standards Institution. BS EN 196-1. (2016). Methods of testing cement. Determination of strength. BSI, London, UK.

British Standards Institution. BS EN 196-6. (2018). Methods of testing cement. Determination of fineness. BSI, London, UK.

Carlson ET and Berman HA. (1960). Some observations on the calcium aluminate carbonate hydrates. Journal of Research of the National Bureau of Standards — A. Physics and Chemistry **64A** 333–341.

Cement, Concrete and Aggregates, Australia. (2018). Ground slag properties, characterisation and uses. Technical Note 78, 12 p.

Chang J and Fang Y. (2015). Quantitative analysis of accelerated carbonation products of the synthetic calcium silicate hydrate (C–S–H) by QXRD and TG/MS. Journal of Thermal Analysis and Calorimetry Vol 119, pp. 57–62.

Concrete Society. (2011). Cementitious materials: the effect of GGBS, fly ash, silica fume and limestone fines on the properties of concrete. Technical Report 74. Concrete Society, Camberley, Surrey, UK, 70 p.

Dinger DR, Funk JE jr. and Funk JE sr. (1982). Rheology of a high solids coal-water mixture; In Proceedings of the 4th International Symposium of Coal Slurry Combustion, Orlando, FL, USA, Vol 4.

Dyer TD. (2014). Concrete Durability. CRC Press, Taylor & Frances Group. Boca Raton, FL, USA, 431 p.

Favier A, De Wolf C, Scrivener K and Habert G. (2018). A sustainable future for the European cement and concrete industry. Project commissioned by European Climate Foundation, Swiss Federal Institutes of Technology Zurich and Lausanne, 93 p.

Funk JE and Dinger DR. (1994). Predictive process control of crowded particulate suspension, applied to ceramic manufacturing. Kluwer Academic Press, New York.

Gupta SC and Larson WE. (1979). A model for predicting packing density of soils using particle-size distribution. Soil Science Society of America Journal, Vol 43, pp. 758–764.

Jianga Y, Linga T-C, Shia C and Panb S-Y. (2018). Characteristics of steel slags and their use in cement and concrete — A review. Resources, Conservation & Recycling, Vol 136, pp. 187–197.

Kondraivendhan B and Bhattacharjee B. (2010) Effect of age and water-cement ratio on size and dispersion of pores in ordinary Portland cement paste. ACI Materials Journal, Vol 107, pp. 147–154.

Matthes W, Vollpracht A, Villagrán Y, Kamali-Bernard S, Hooton D, Gruyaert E, Soutsos M and De Belie N. (2017). Ground granulated blast furnace slag. Properties of fresh and hardened concrete containing supplementary cementitious materials: State-of-the-art Report of the RILEM Technical Committee 238-SCM, WG 4, Vol 25/1, Eds. Nele De Belie, Marios Soutsos, Elke Gruyaert, pp. 1–54.

Mayes WM, Riley AL, Gomes HI, Brabham P, Hamlyn J, Pullin H and Renforth P. (2018). Atmospheric CO_2 sequestration in iron and steel slag: Consett, County Durham, United Kingdom. Environmental Science and Technology, Vol 52, pp. 7892–7900.

McCarthy MJ, Robl TL and Csetenyi LJ. (2017). Recovery, processing, and usage of wet-stored fly ash. Chapter 14, Coal combustion products (CCP's) - characteristics, utilization and beneficiation (Eds. Robl, Oberlink and Jones), Elsevier, Oxford, UK, pp. 343–368.

McCarthy MJ, Zheng L, Dhir RK and Tella G. (2018). Dry-processing of long-term wet-stored fly ash for use as an addition in concrete. Cement and Concrete Composites, Vol 92, pp. 205–215.

Meng B. (1994). Calculation of moisture transport coefficients on the basis of relevant pore structure parameters. Materials and Structures, Vol 27, pp. 125–134.

Mineral Products Association. (2015). Embodied CO_{2e} of UK cement, additions and cementitious material. Fact Sheet 18, http://cement.mineralproducts.org/documents/Factsheet_18.pdf, 8 p, (last accessed, 12 June 2017).

Page RJ and Fanourakis GC. (2008). The influence of slag fineness on the workability of cementitious pastes. Concrete / Beton, Vol 120, pp. 6–12.

Paine KA, Dhir RK and Zheng L. (2006). Predicting early-age temperatures of blended-cement concrete. Proceedings of Institution of Civil Engineers, Construction Materials, Vol 159, pp. 163–170.

Rhodes C. (2018). UK steel industry: statistics and policy. Briefing Paper No 07317, January 2018, The House of Commons Library Research Service, 30 p.

Robl TL, Groppo JG, Jackura A and Tapp K. (2006). Field testing of an advanced multi-product coal by-product processing plant at Kentucky Utilities Ghent Power Plant. Ashtech 2006, Birmingham, 2006, 7 p.

Scott PW, Critchley SR and Wilkinson FCF. (1986). The chemistry and mineralogy of some granulated and pelletized blast furnace slags. Mineralogical Magazine, Vol 50, pp. 141–147.

Thomas MDA. (2013). Supplementary cementing materials in concrete. CRC Press, Taylor & Frances, Boca Raton, FL, USA, 179 p.

TRB (Transportation Research Board). (2013). Research Results Digest 382: Measuring Cement Particle Size and Surface Area by Laser Diffraction. TRB, Washington, DC, USA.

Webb TL and Heystek H. (1957). The carbonate minerals. In: The differential thermal investigation of clays (Mackenzie, R. (ed.)), Mineralogical Society, London, 1957, pp. 329–363.

Yildirim IZ and Prezzi M. (2011). Chemical, mineralogical, and morphological properties of steel slag. Advances in Civil Engineering, Vol 2011, Article ID 463638, 13 p.

Yildirim IZ and Prezzi M. (2015). Geotechnical properties of fresh and aged basic oxygen furnace steel slag. Journal of Materials in Civil Engineering, Vol 17, 04015046.

Table 1. Characteristics of the Portland cement (CEM I) used in the study (Data from Supplier)

CHARACTERISTIC	**CEM I**
Oxide Composition, % by mass	
CaO	63.4
SiO_2	19.2
Al_2O_3	4.8
Fe_2O_3	2.7
MgO	1.0
Na_2O	0.2
K_2O	0.7
SO_3	3.2
Cl	0.06
LOI	3.5
Clinker compound, % by mass	
C_3S	63.0
C_2S	14.3
C_3A	6.9
C_4AF	7.2
Physical properties	
Fineness, m^2/kg	410
Setting time, initial, mins.	150
Strength class	52.5N

Table 2. Chemical composition of the fresh and weathered slags used in the study

CONSTITUENT	QUANTITY, % BY MASS	
	Fresh slag	**Weathered slag**
CaO	37.92	37.70
SiO_2	34.66	34.04
Al_2O_3	10.33	9.87
Fe_2O_3	0.32	0.38
MgO	7.38	7.19
TiO_2	0.86	0.62
MnO	0.21	0.23
Na_2O	0.32	0.19
K_2O	0.46	0.44
SO_3	1.59	1.97
Cl	0.02	0.01
LOI	0.73	1.97

Table 3. Specific surface area of the slag samples measured using Blaine air permeability, BET nitrogen adsorption and laser diffraction (cm^2/g)

MATERIAL	BLAINE	BET NITROGEN ADSORPTION	LASER DIFFRACTION
Fresh Slag	3830	12530	3800
Weathered Slag 1	3820	11630	3060
Weathered Slag 2	3780	12190	3360

Table 4. Results of flow measurements conducted on the fresh mortars

MIX TYPE	SLAG TYPE	FLOW DIAMETER, mm
100% PC	-	217.6
50% PC / 50% Slag	Fresh	215.4
	Weathered 1	221.3
	Weathered 2	214.9

Table 5. Porosity of mortars made from the slags investigated

MIX TYPE	SLAG TYPE	POROSITY, ml/g		
		≥10 nm	**<10 nm**	**Total**
100% PC		0.0463	0.0025	0.0488
50% PC / 50% Slag	Fresh	0.0363	0.0020	0.0383
	Weathered 1	0.0715	0.0046	0.0761
	Weathered 2	0.0639	0.0043	0.0682

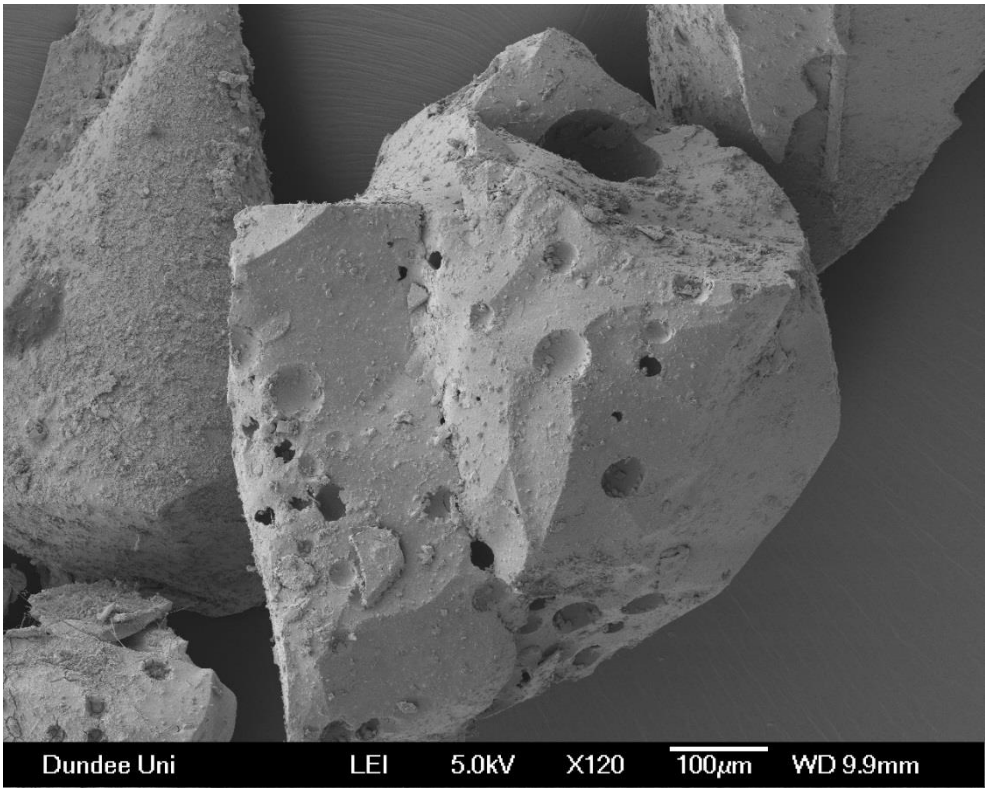

(a)

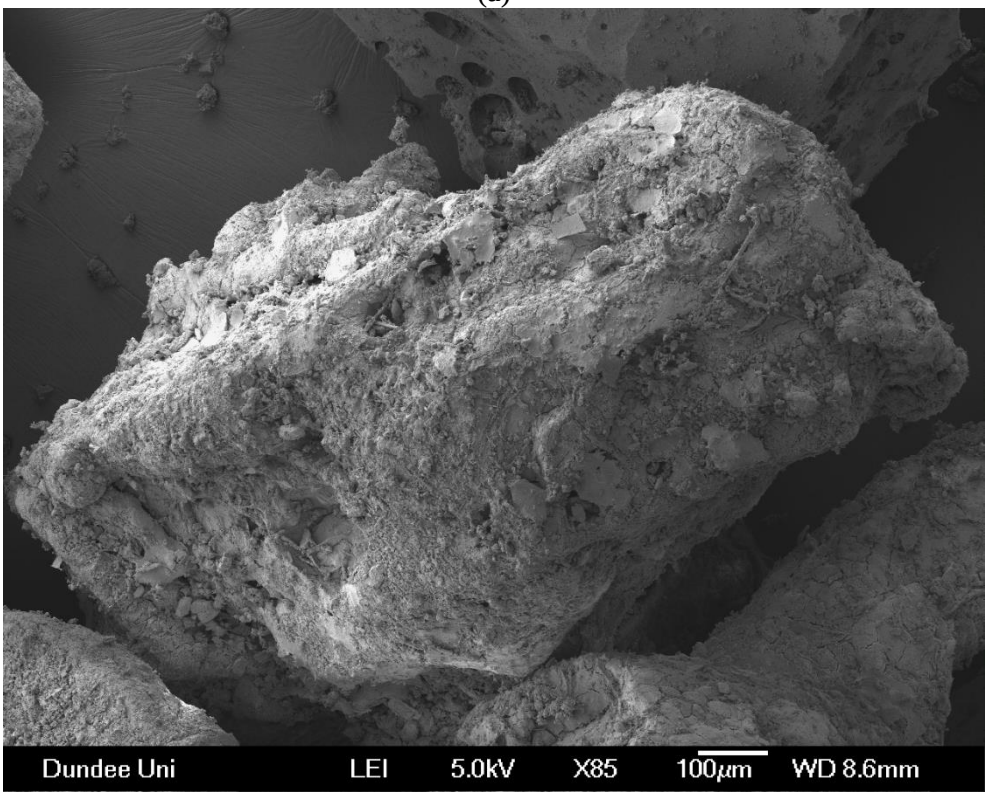

(b)

Figure 1. Scanning electron microscopy image of granules of (a) fresh blast furnace slag ×120 and (b) weathered blast furnace slag ×85

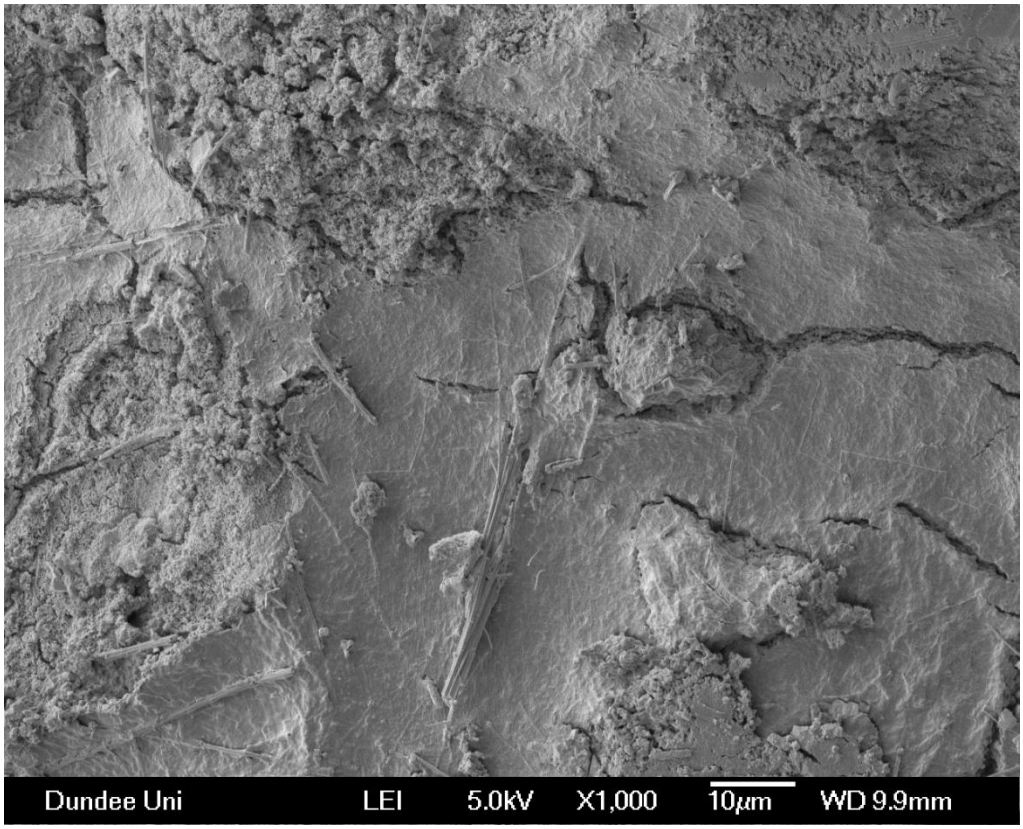

(a)

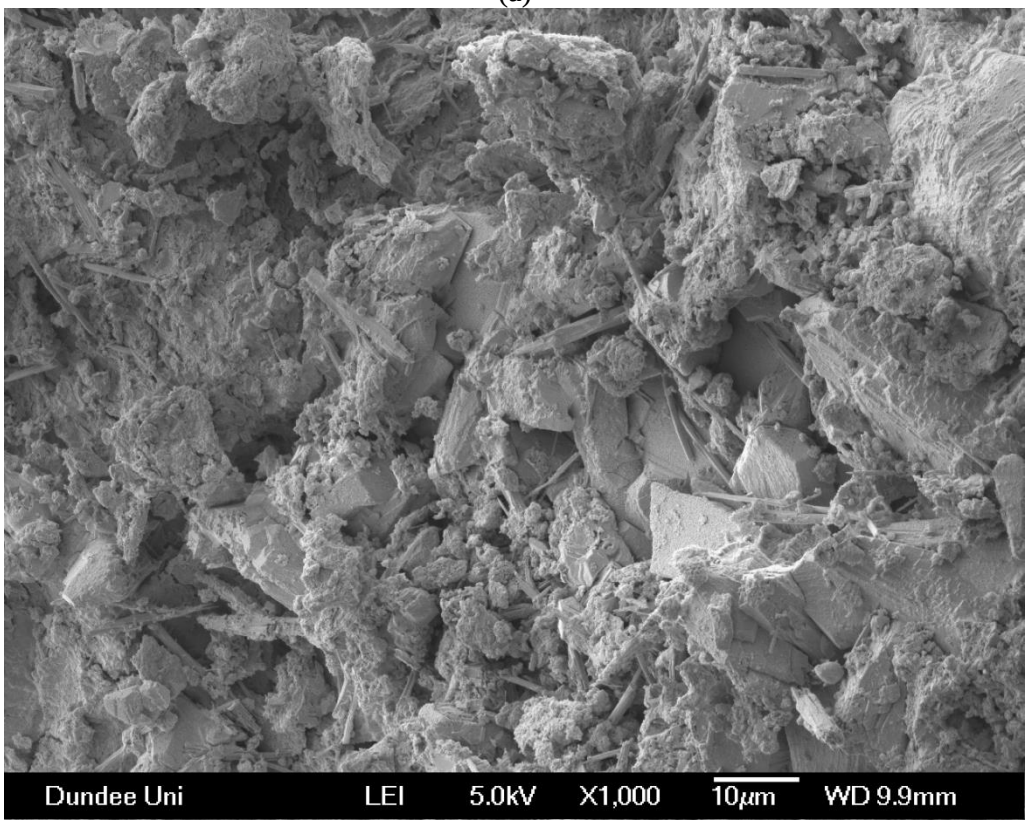

(b)

Figure 2. Scanning electron microscope image of the surface of a granule of (a) fresh blast furnace slag ×1000 and (b) weathered blast furnace slag ×1000

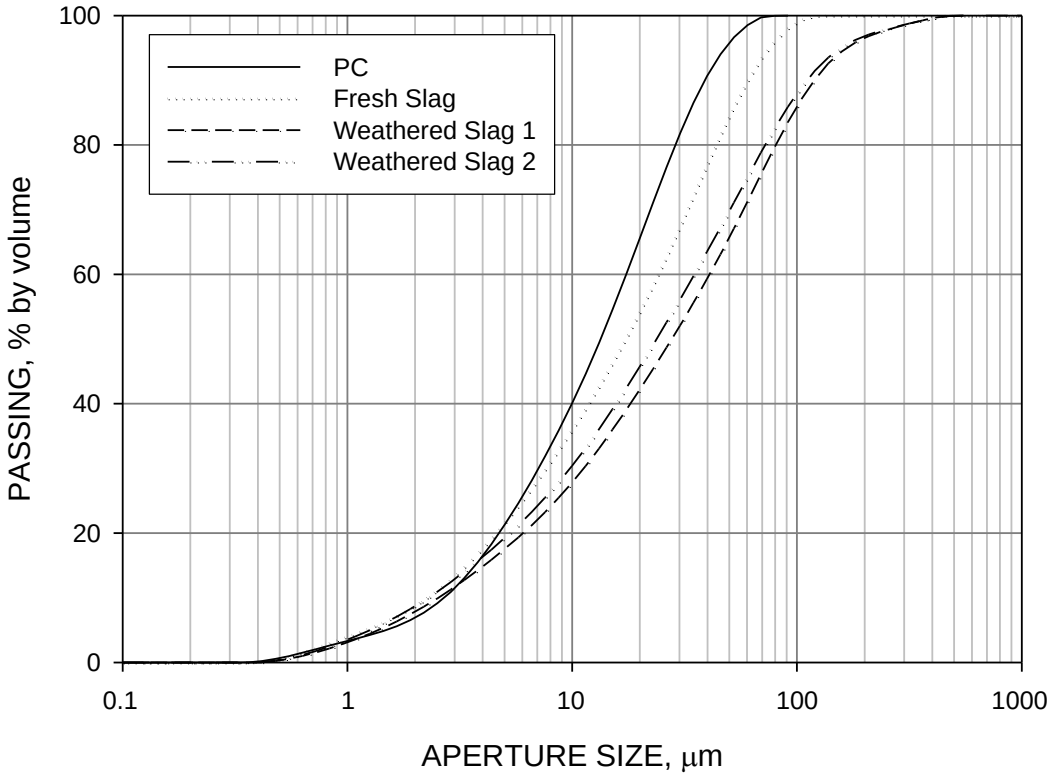

Figure 3. Cumulative particle size distributions of the fresh and weathered slags after grinding

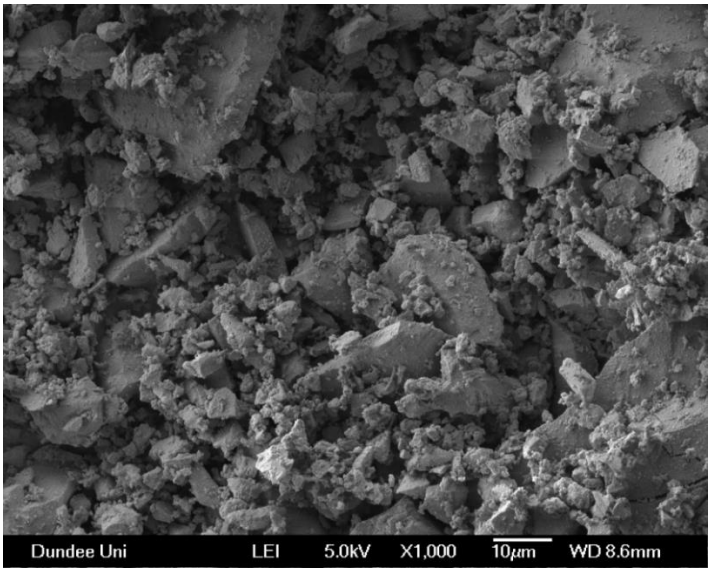

(a)

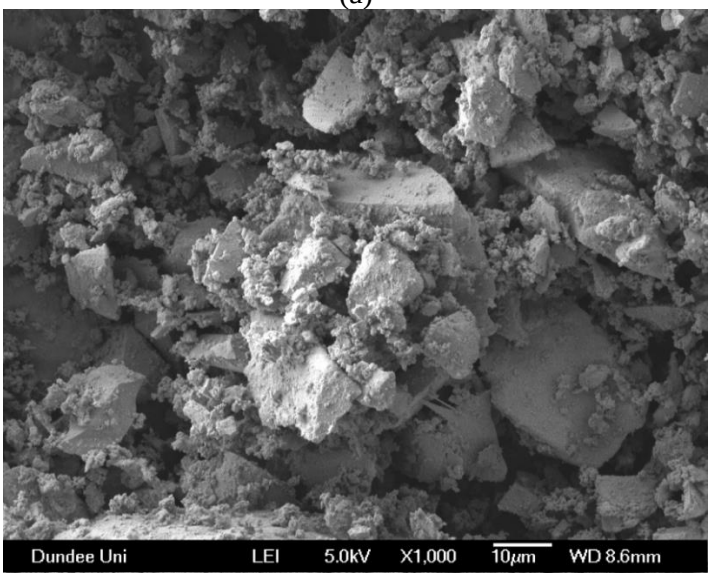

(b)

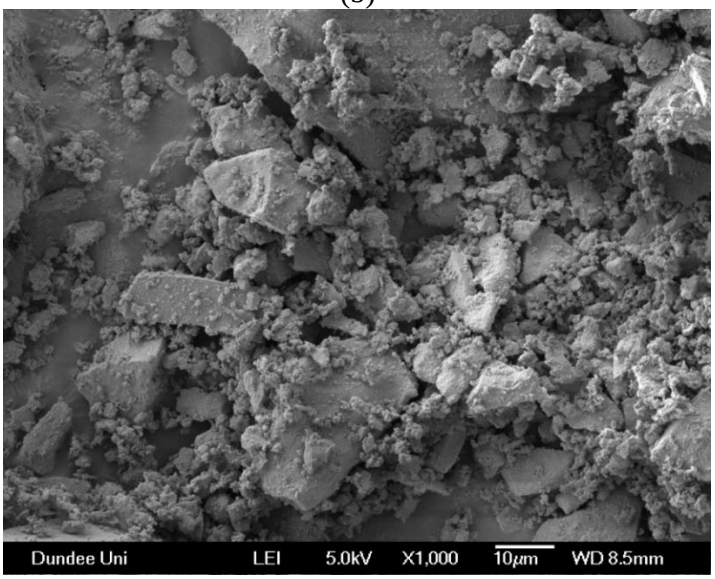

(c)

Figure 4. The slag samples after grinding (a) fresh slag, (b) weathered slag 1 and (c) weathered slag 2

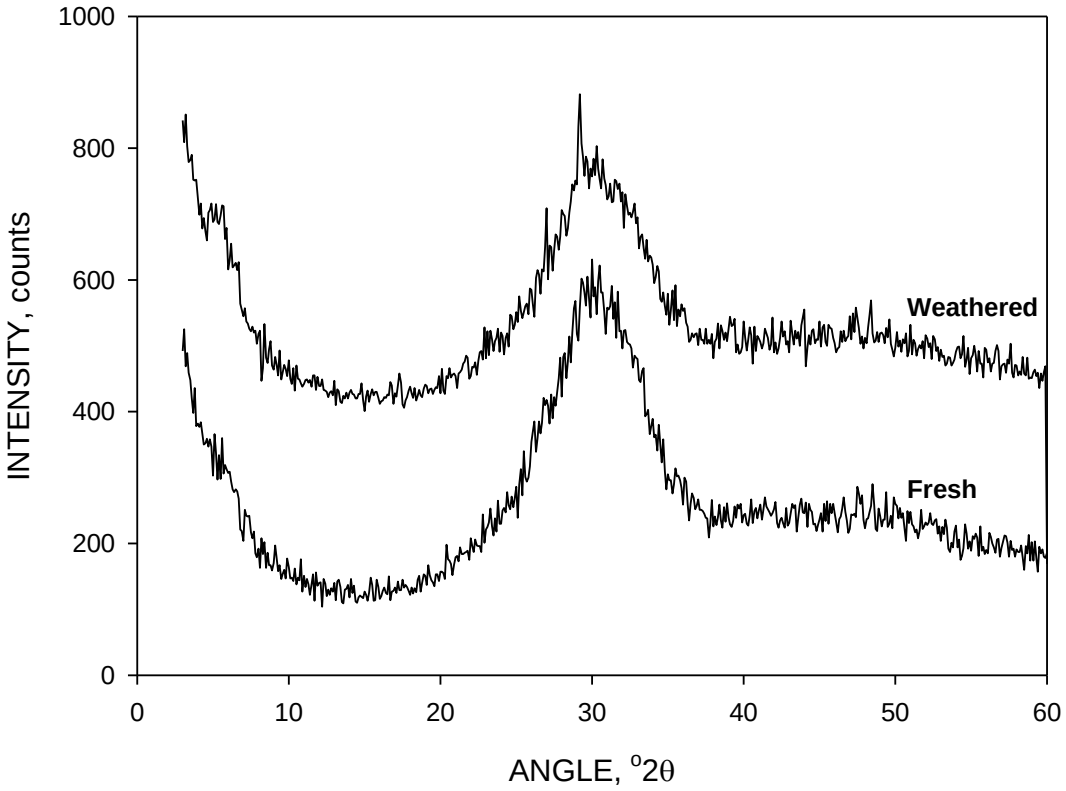

Figure 5. Powder X-ray diffraction traces from the fresh and weathered slags

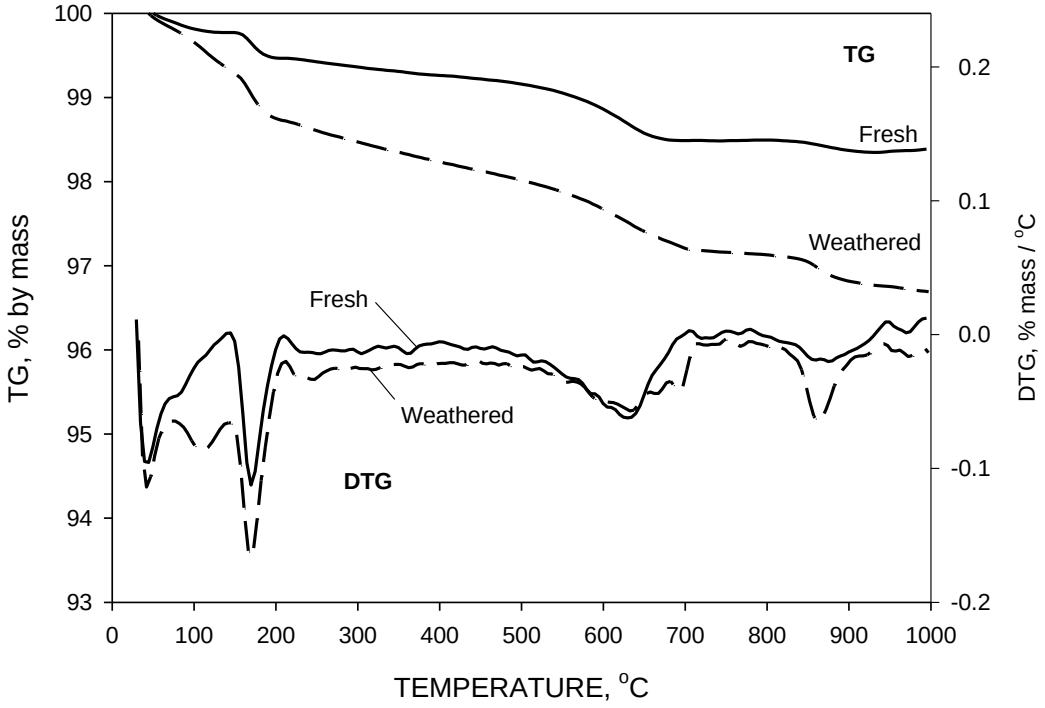

Figure 6. Thermogravimetry (TG) and differential thermogravimetry (DTG) plots from the fresh and weathered slag samples after grinding

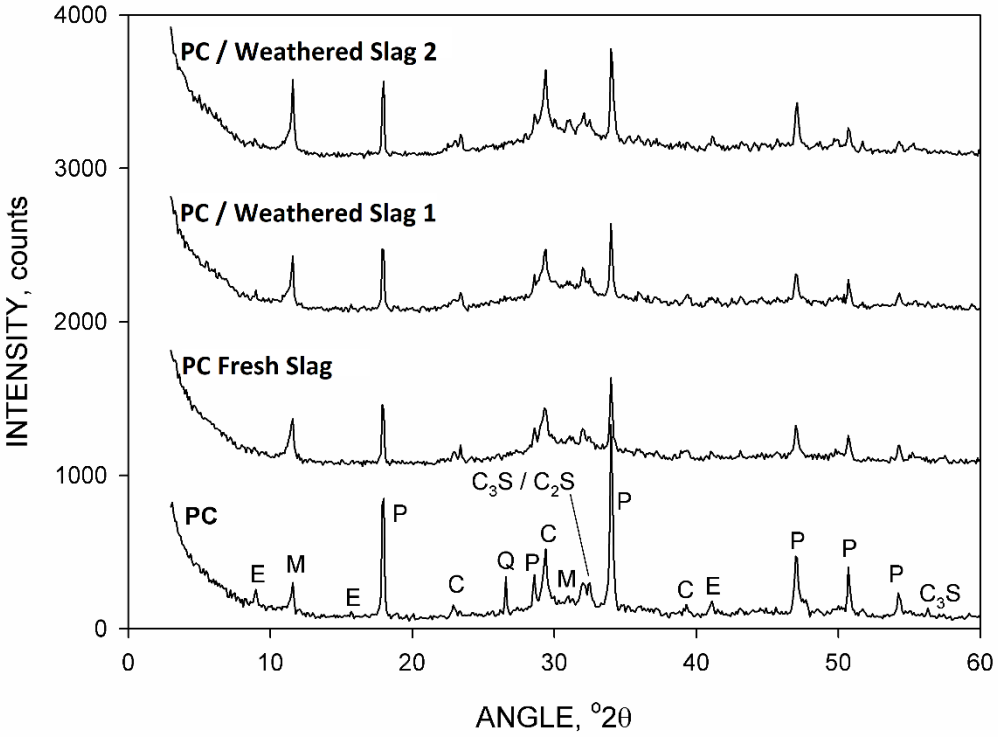

Figure 7. XRD traces from the 28-day paste specimens. E = ettringite, M = calcium aluminate monocarbonate hydrate, P = portlandite, C = calcite, C_3S = tricalcium silicate, C_2S dicalcium silicate

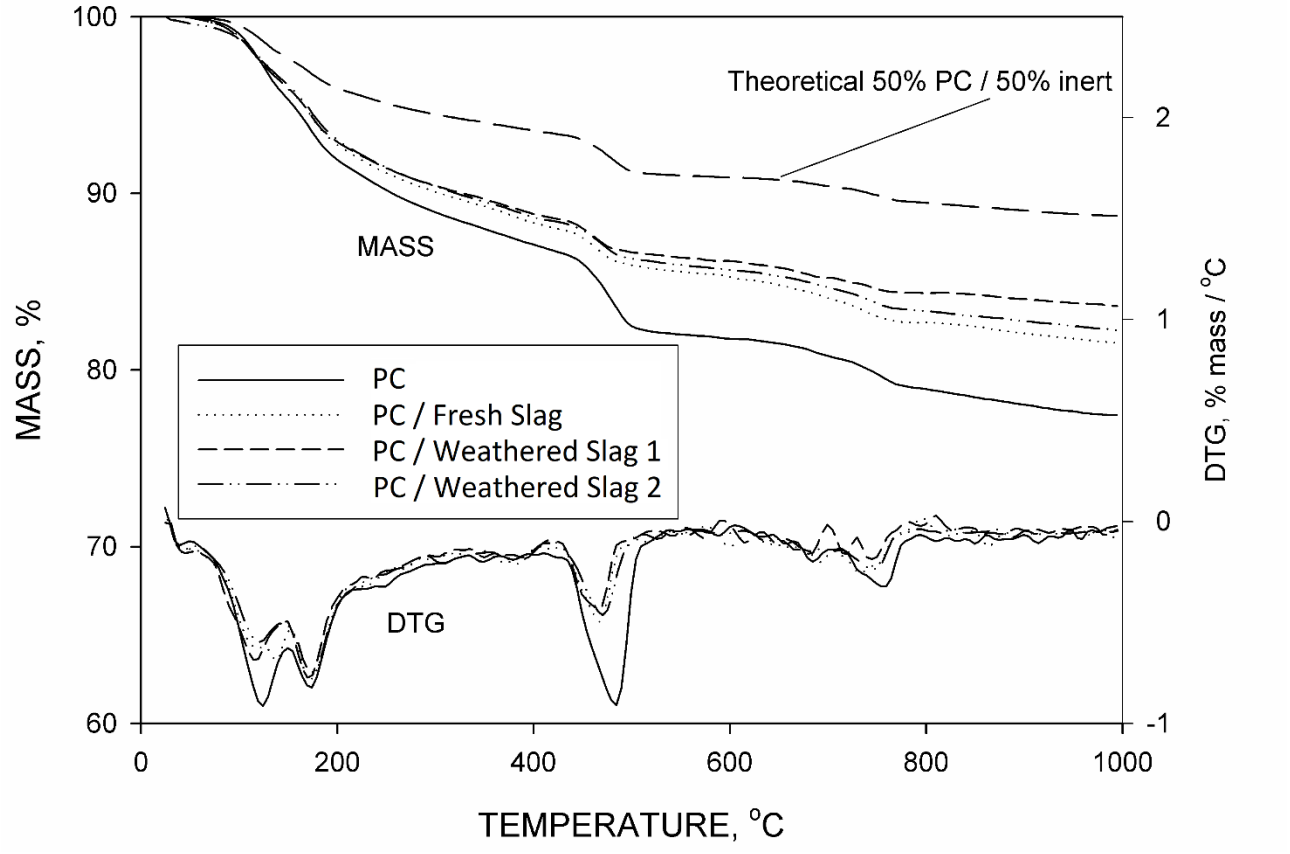

Figure 8. TG traces from the 28-day paste specimens

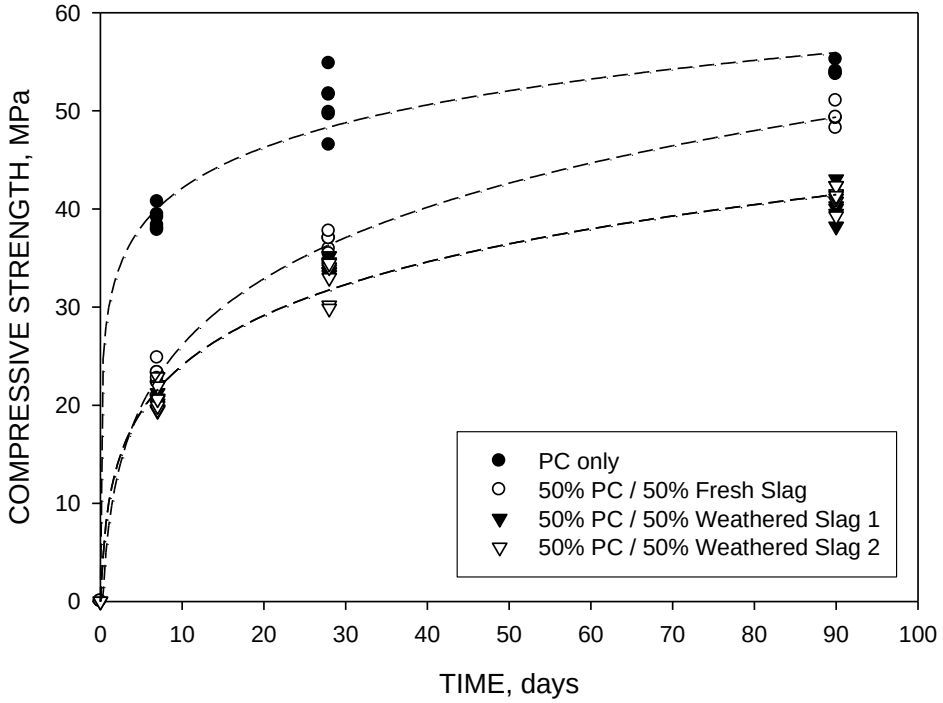

Figure 9. Strength development of the mortars

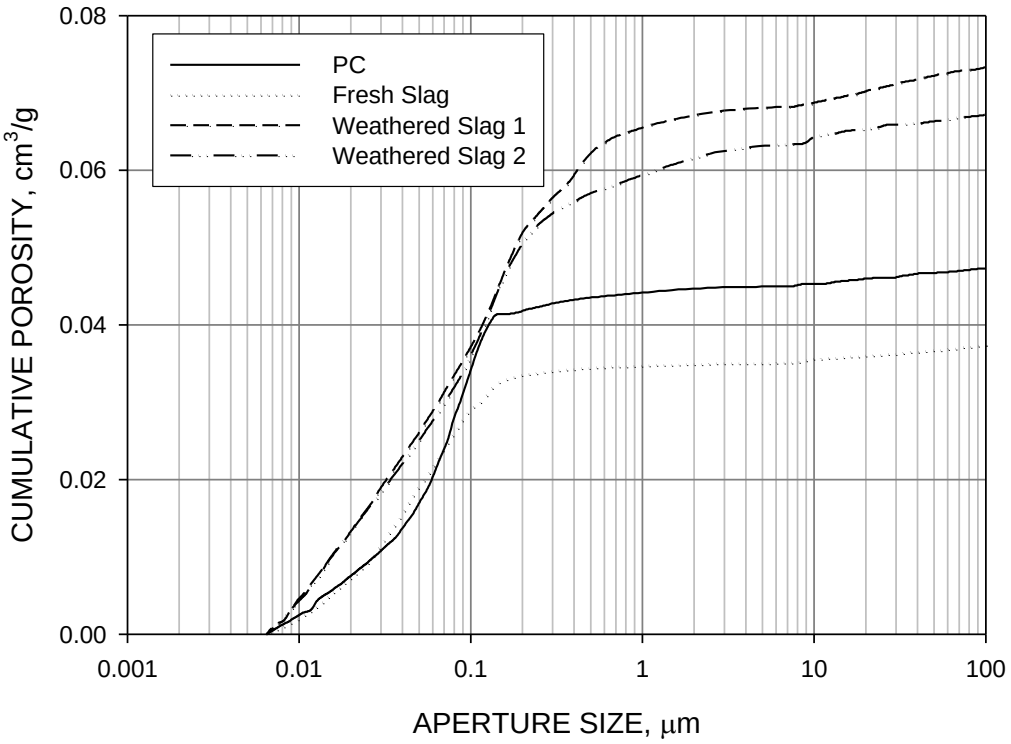

Figure 10. Cumulative pore size distributions of the 28-day mortars

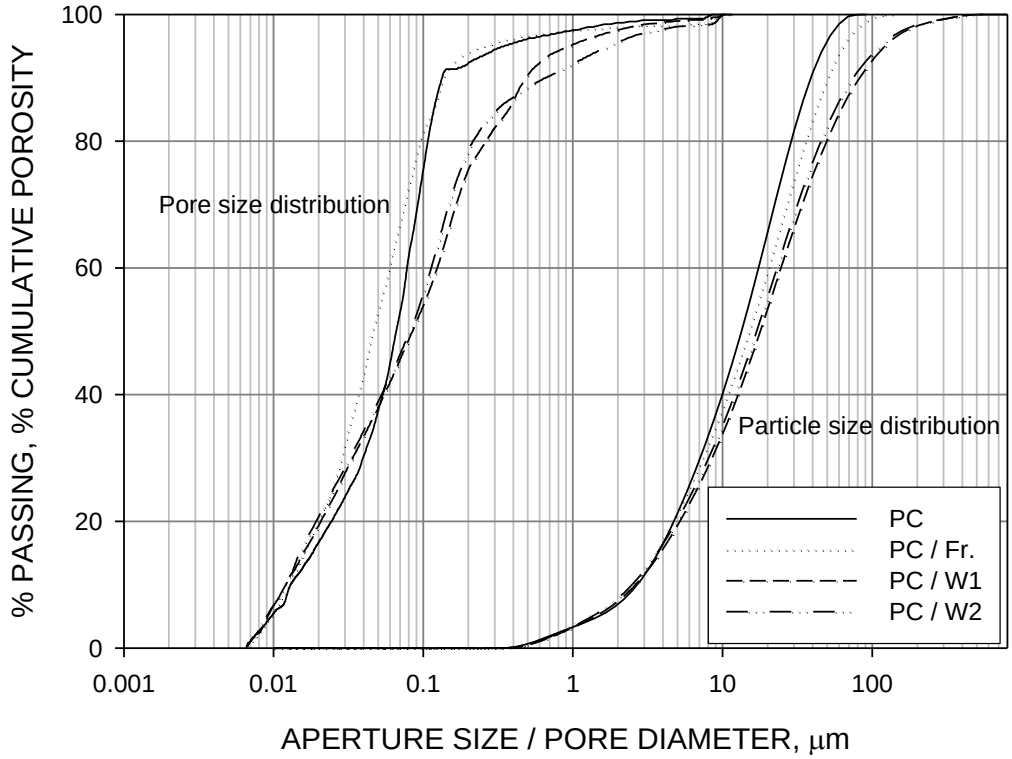

Figure 11. Comparison of calculated particle size distributions of the cement formulations and the pore size distributions of the mortars. Fr = fresh slag, W1, W2 = weathered slag